



# Nuclear matter property based on the TDDFT

**Yoritaka Iwata**

Institute of Innovative Research, Tokyo Institute of Technology  
Department of Mathematics, Shibaura Institute of Technology

REF. J. Stone, P. Danielewicz, and Y. Iwata, *PHYSICAL REVIEW C* **96**, 014612 (2017)

This talk is an introductory guide to **the recent paper**

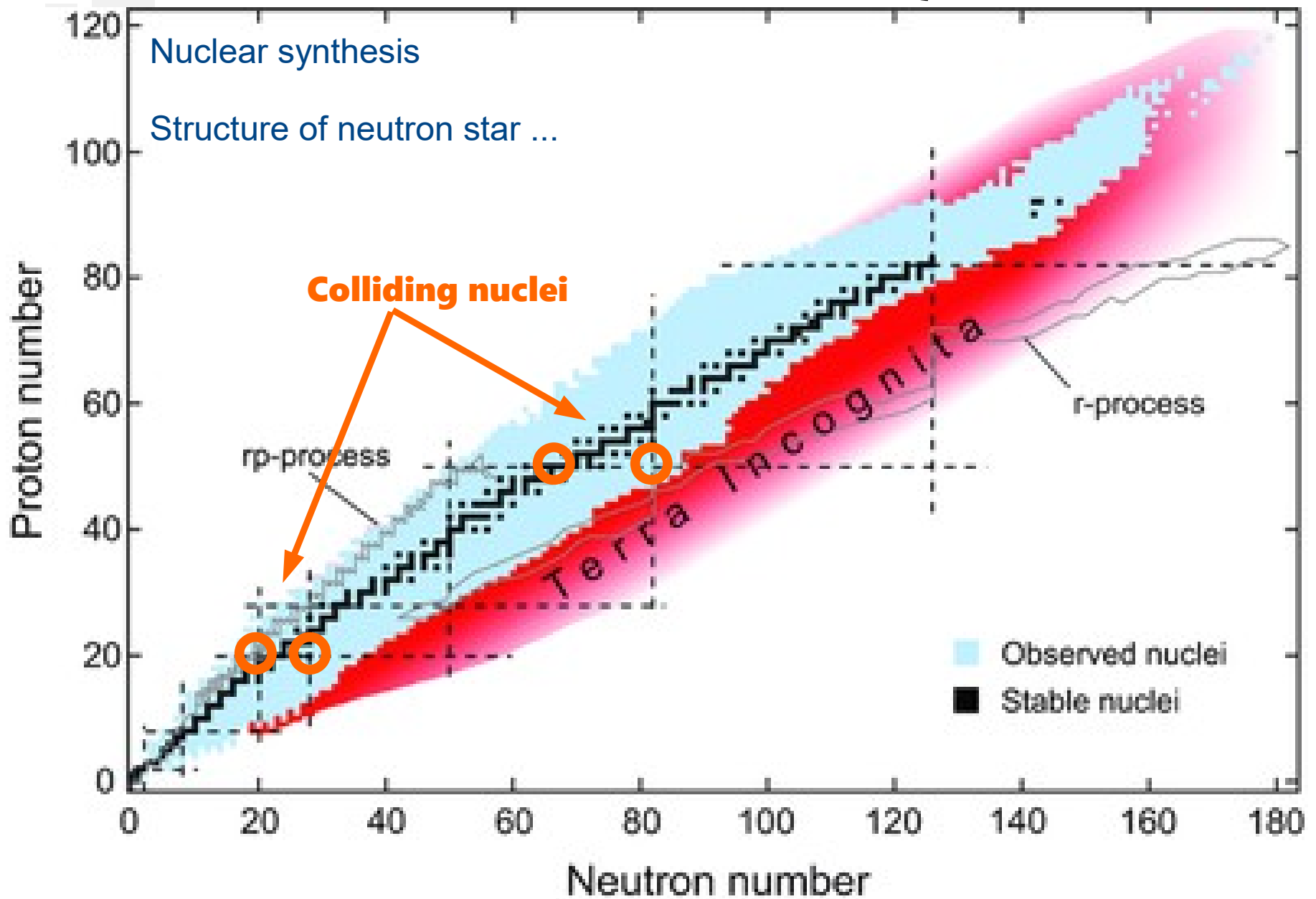
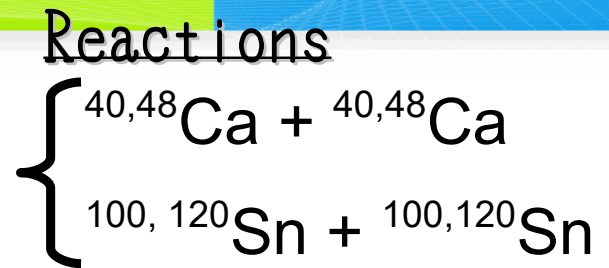
“J. Stone, P. Danielewicz, and Y. Iwata, PRC **96**, 014612 (2017)”

from a view of TDHF approach

# Contents

- ◇ Introduction - symmetry energy -
- ◇ TDHF and  $p$ -BUU
- ◇ Maximal density at low and higher energy cases
- ◇ Summary

# Introduction on chart



# Introduction

## -Symmetry energy-

Zero temp. formalism

$$\mathcal{E}(\rho, \delta) = \underbrace{\mathcal{E}(\rho, \delta = 0)}_{\dots \text{ symmetry matter}} + S(\rho) \delta^2 \quad \leftarrow \text{Energy per nucleon (expanded by } \delta)$$

$$\delta = (\rho_n - \rho_p) / \rho \quad \leftarrow \text{proton-neutron asymmetry (local density difference)}$$

### Symmetry energy

$$S(\rho) \equiv \frac{1}{2} \frac{\partial^2 \mathcal{E}(\rho, \delta)}{\partial \delta^2} \Big|_{\delta=0} \approx \mathcal{E}(\rho, \delta = 1) - \mathcal{E}(\rho, \delta = 0)$$

$$S(\rho) = S_{\text{kin}}(\rho) + S_{\text{int}}(\rho) = 12.3 \text{ MeV} \left( \frac{\rho}{\rho_0} \right)^{2/3} + S_{\text{int}}(\rho)$$

Maximal density  $\rightarrow$  symmetry energy  
(energy dep ...)

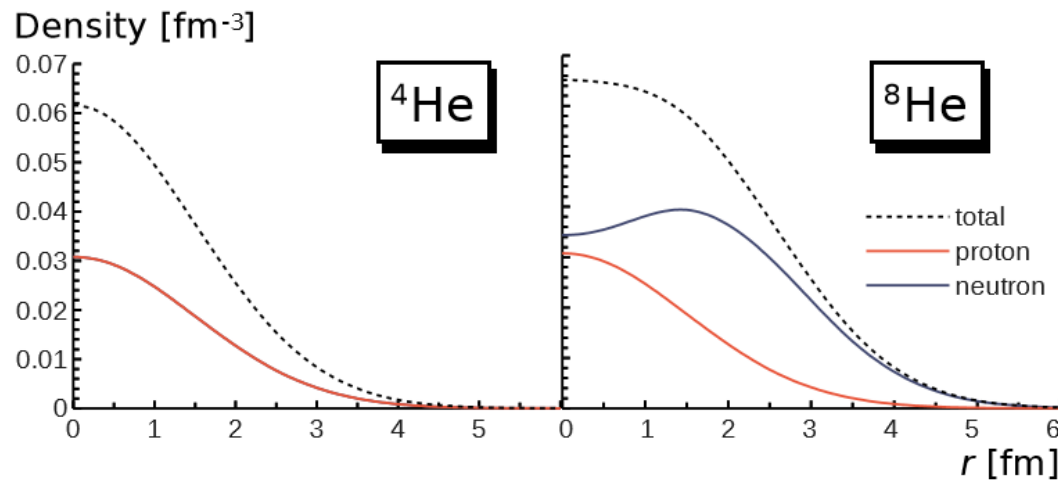
# Interaction Parameter

TABLE I. Adjustable parameters in the pBUU and TDHF models.

Model	Parameter group	Parameter	Value	
pBUU	Gradient term in energy $E_1$	$a_1$	21.4 MeV fm <sup>2</sup>	
		Density dependent contribution to mean field $U_\rho$	$a$	209.791 MeV
			$b$	69.7571 MeV
			$v$	1.46226
			$\rho_0$	0.160 fm <sup>-3</sup>
			$K$	210 MeV
		Momentum dependent contribution to mean field $\delta U_p$	$c$	0.645700
			$\lambda$	0.954605
			$m^*/m$	0.70
		Interaction contribution to symmetry energy $S_{\text{int}}$	$s_0$	20.0 MeV
			$s_1$	50.1 MeV
			$s_2$	31.9 MeV
			$s_3$	1.47
		In-medium cross section Eqs. (11) and (12) of Ref. [23]	$v_{\text{cs}}$	0.667
Monte Carlo integration			$\mathcal{N}_Q$	3000
TDHF model	SV-bas	11 parameters in Ref. [30]		

P. Klupfel, P. G-. Reinhard et al.  
PRC (2009)

# Quality of TDDFT (SV-bas int.)



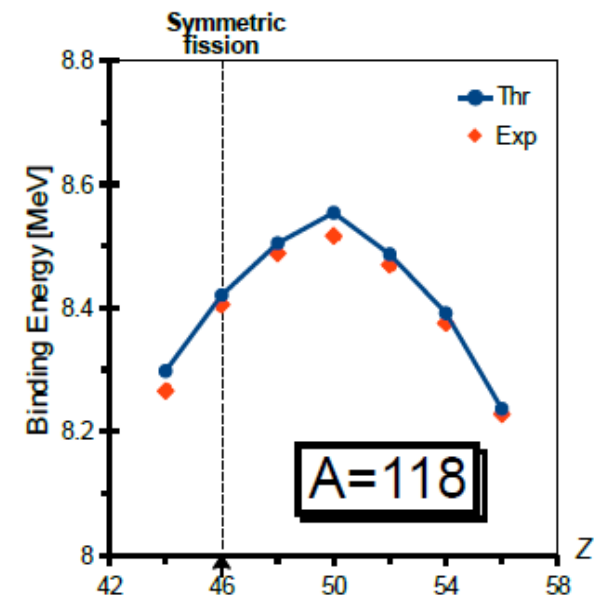
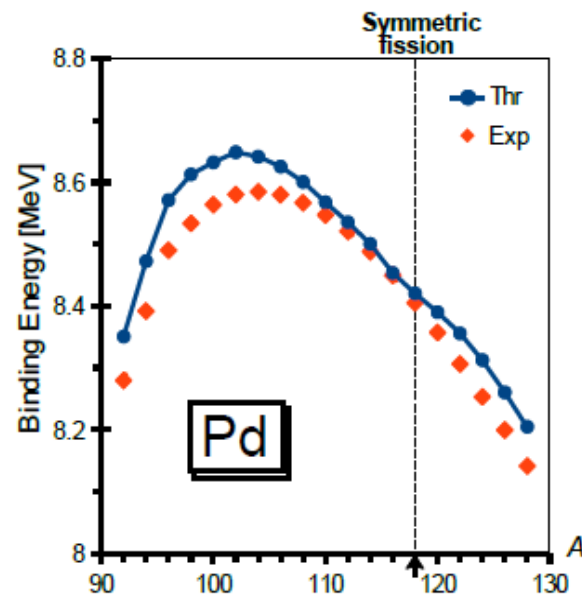
Comparison of RMS radii

The roots of mean square matter radii are ...

<sup>4</sup>He: 1.50 fm by theoretical calculation

(EXP 1.49 to 1.63 fm)

Comparison of binding energy



# Density dependence of symmetry energy

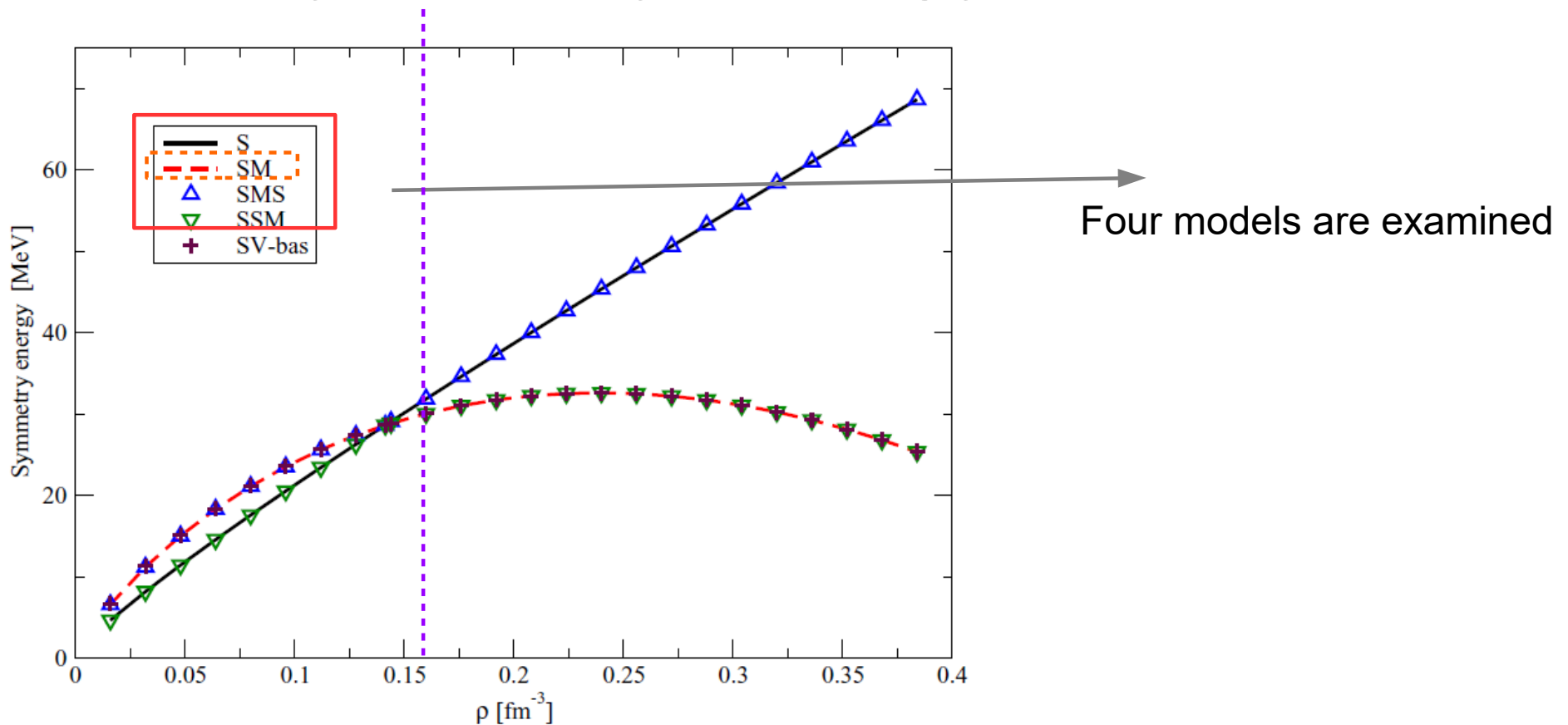
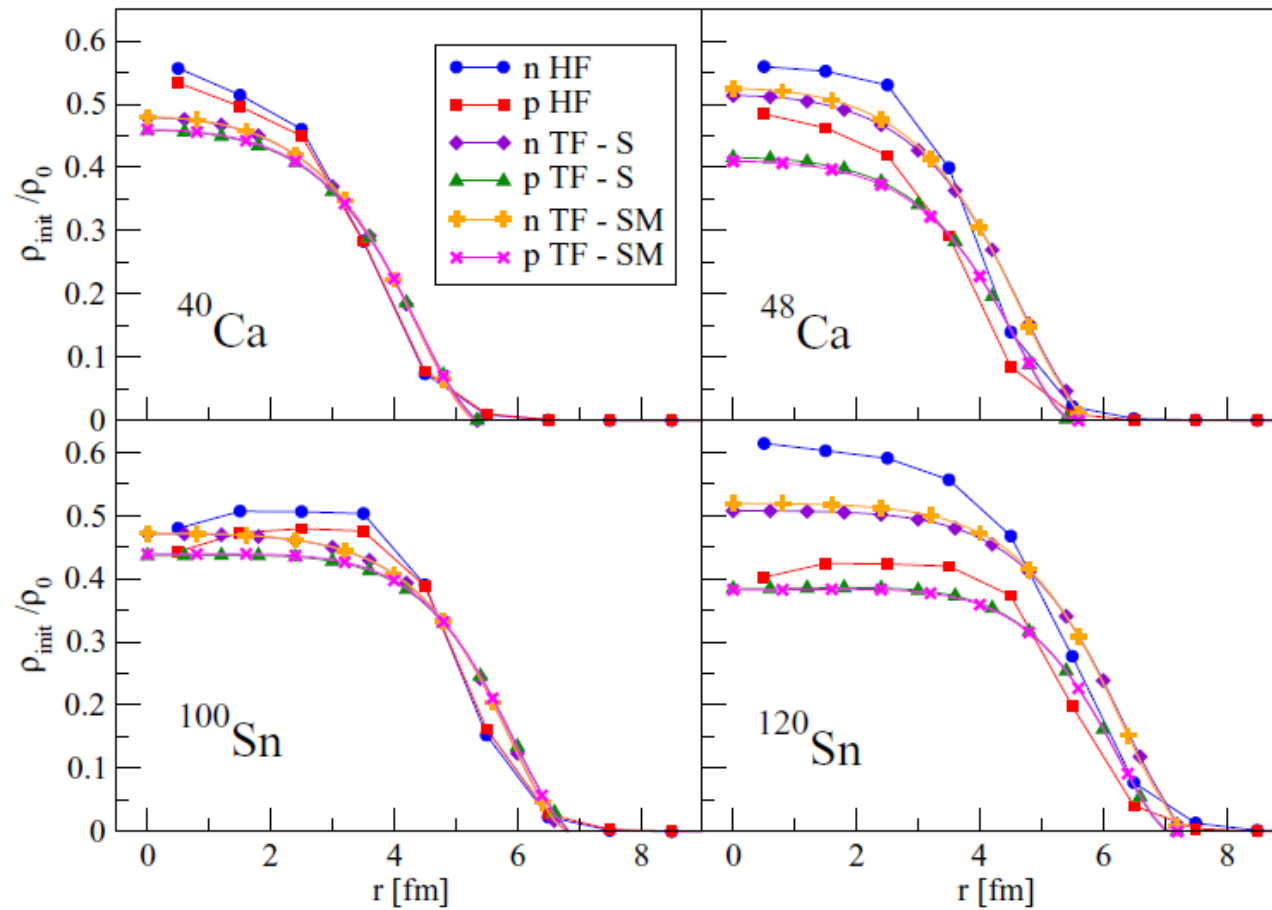


FIG. 1. Density dependence of the symmetry energy in the models employed in this work. The values of the symmetry energy  $S$  and of its slope  $L$ , at  $\rho_0$ , are  $S(L) = 31.8(82.8)$ ,  $30.0(32.4)$ , and  $30.2(32.3)$  MeV, for  $S$  and  $SM$  in pBUU, and for SV-bas, respectively. Models SMS and SSM are added for completeness.

# Neutron and proton density

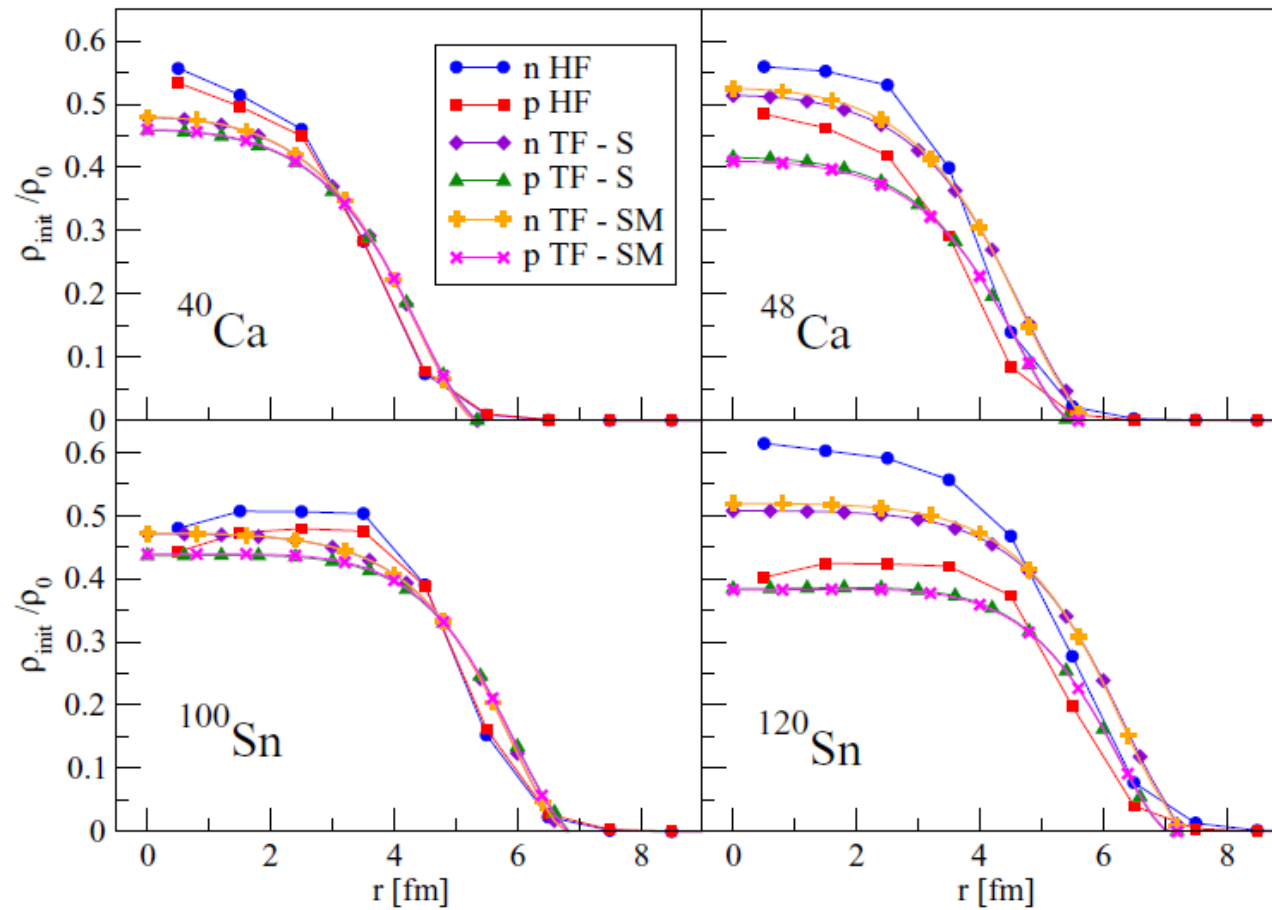


Difference can be found in the **tails**

FIG. 2. Neutron and proton densities as a function of distance from the center of nucleus, for the nuclei considered in the paper, from static HF and TF calculations.



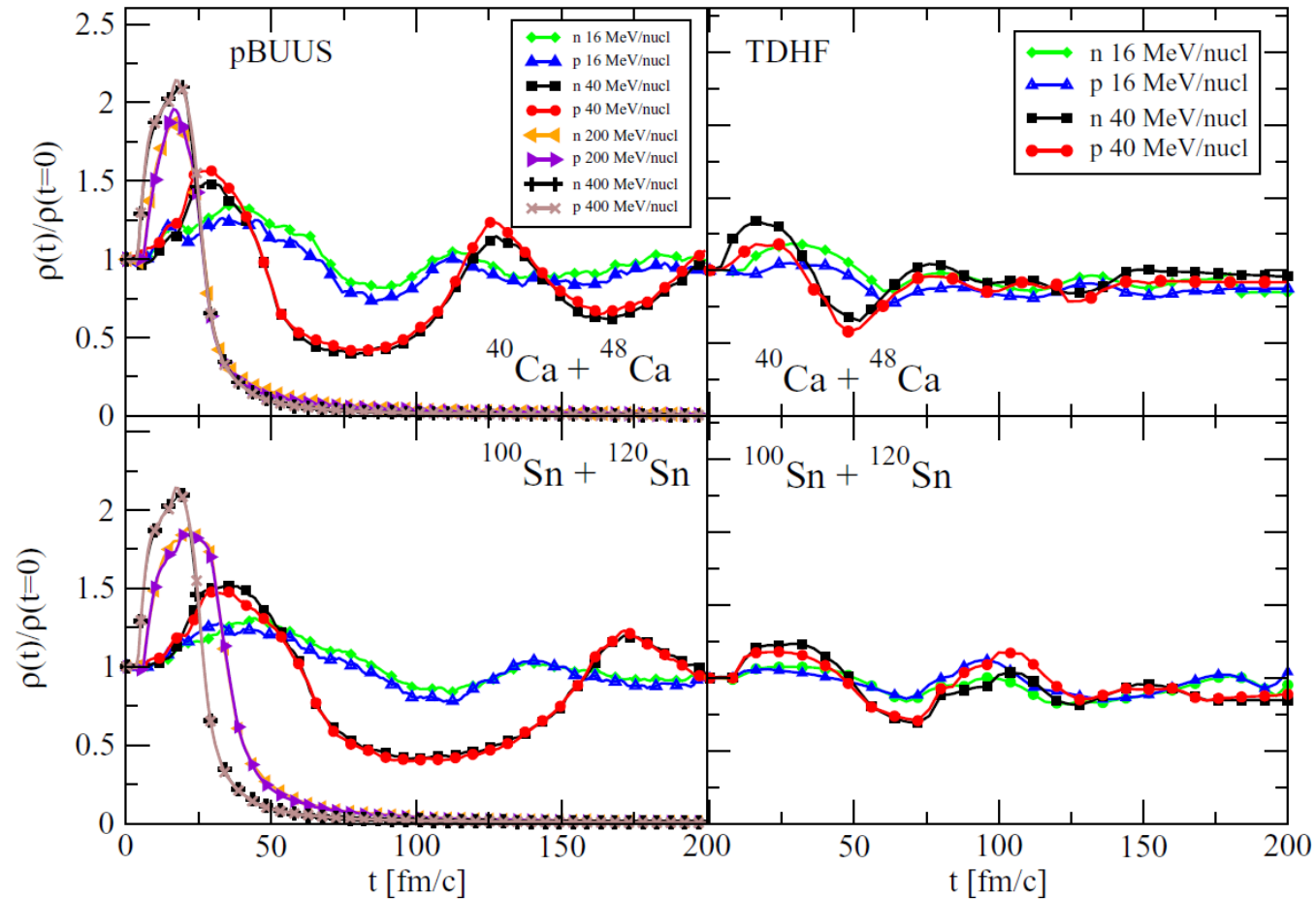
# Neutron and proton density



Difference can be found in the **tails**

FIG. 2. Neutron and proton densities as a function of distance from the center of nucleus, for the nuclei considered in the paper, from static HF and TF calculations.

# Time evolution of maximal density



Maximal density is achieved in the 1<sup>st</sup> full overlaps.

FIG. 3. Time evolution of maximal proton and neutron densities normalized to their static value, in asymmetric collisions,  $^{40}\text{Ca} + ^{48}\text{Ca}$  and  $^{100}\text{Sn} + ^{120}\text{Sn}$ , at different incident energies, within pBUU dynamics for symmetry energy  $S$  (left panels) and in TDHF dynamics (right panels).

# Contour plot of proton and neutron densities

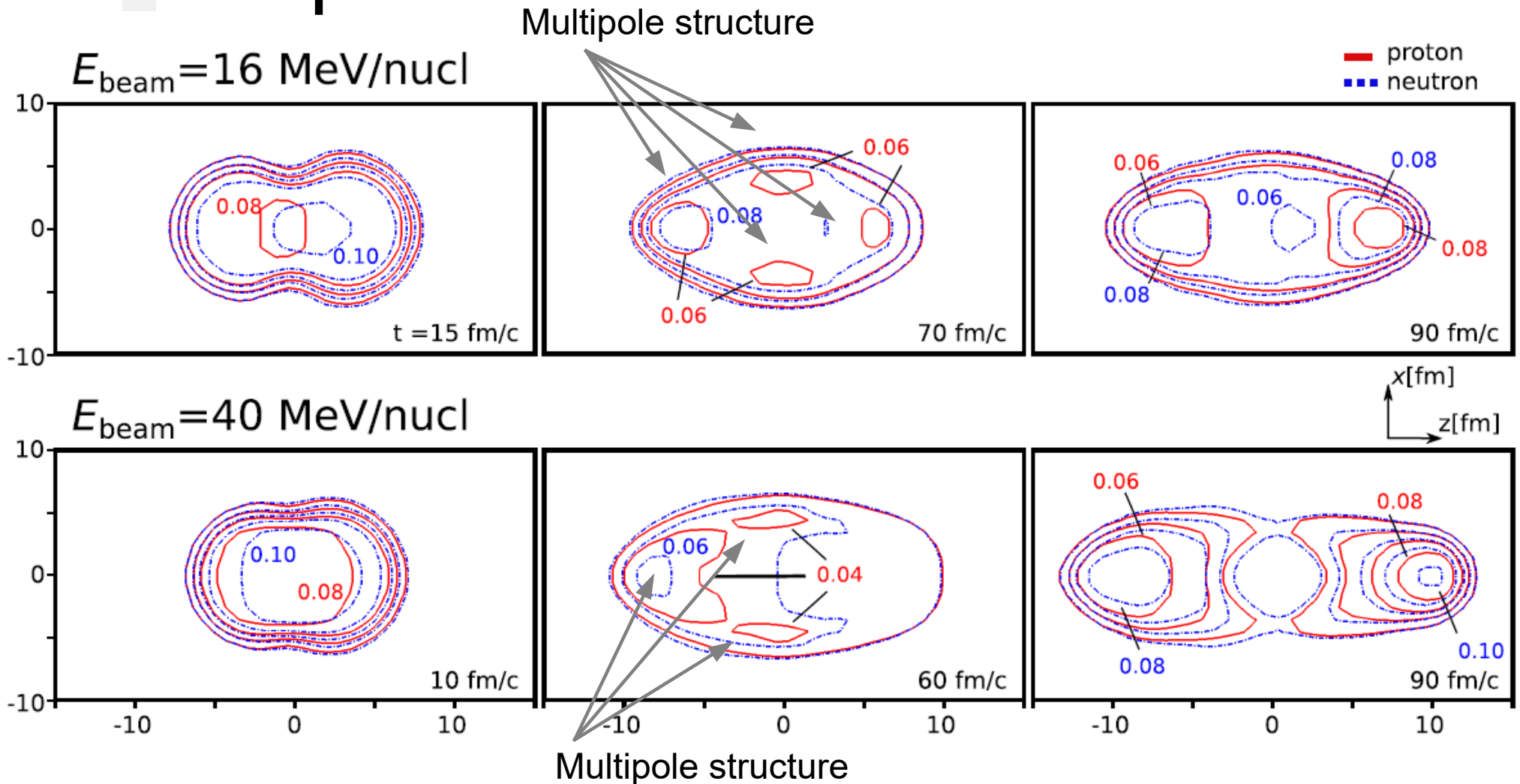


FIG. 4. Contour plots of neutron (dashed lines) and proton density (solid lines) in head-on  $^{120}\text{Sn} + ^{100}\text{Sn}$  collisions at 16 MeV/nucl. (top) and 40 MeV/nucl., at different times. The horizontal axis is the collision axis.

# Maximal density and corresponding $\delta$

Ca cases

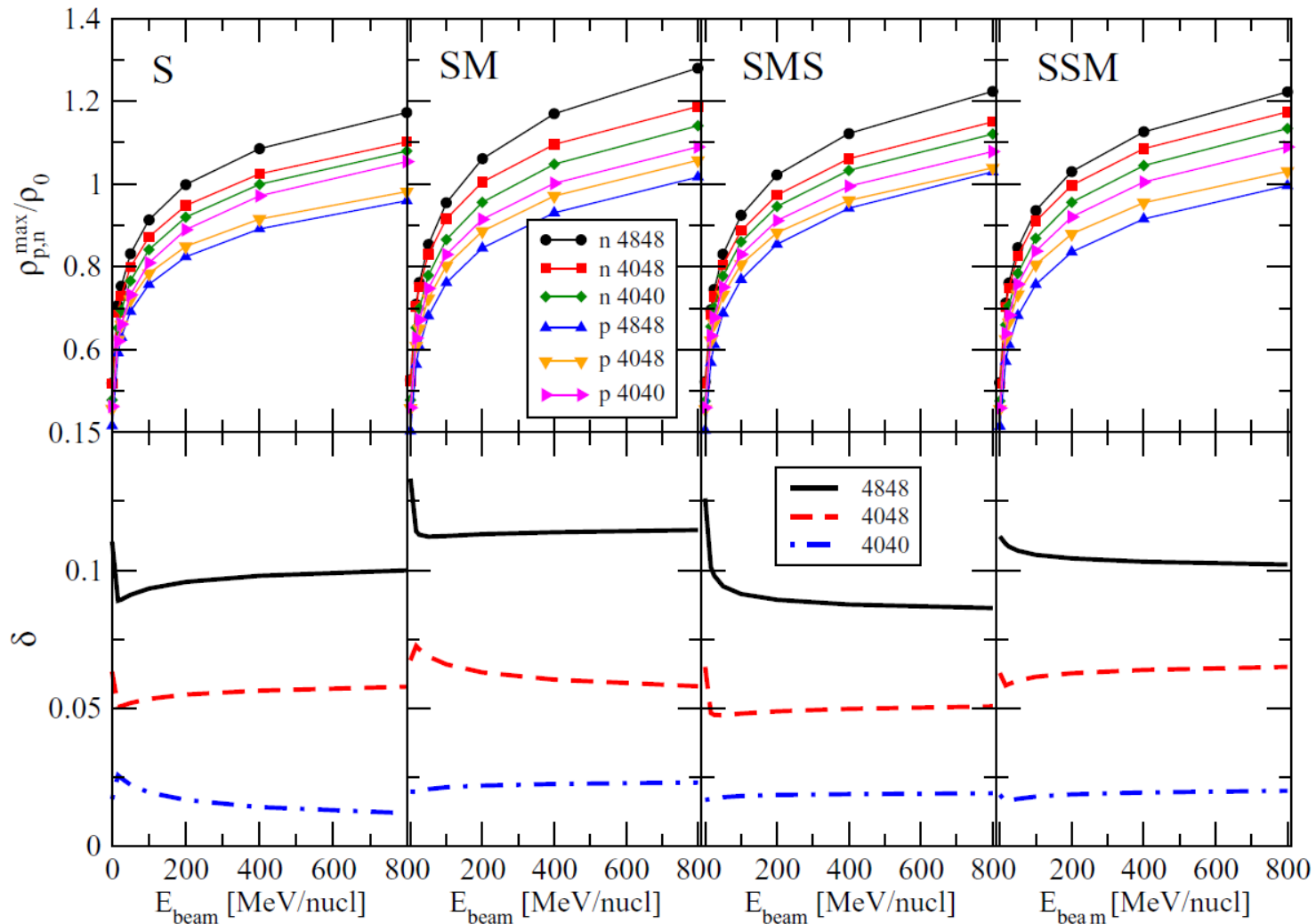


FIG. 5. Maximum neutron and proton densities in units of  $\rho_0$  (top panels) and the corresponding values of the asymmetry  $\delta$  (bottom panels), vs beam energy for Ca systems, yielded in the pBUU simulations with different indicated forms of symmetry energy.

# Maximal density and corresponding $\delta$

Sn cases

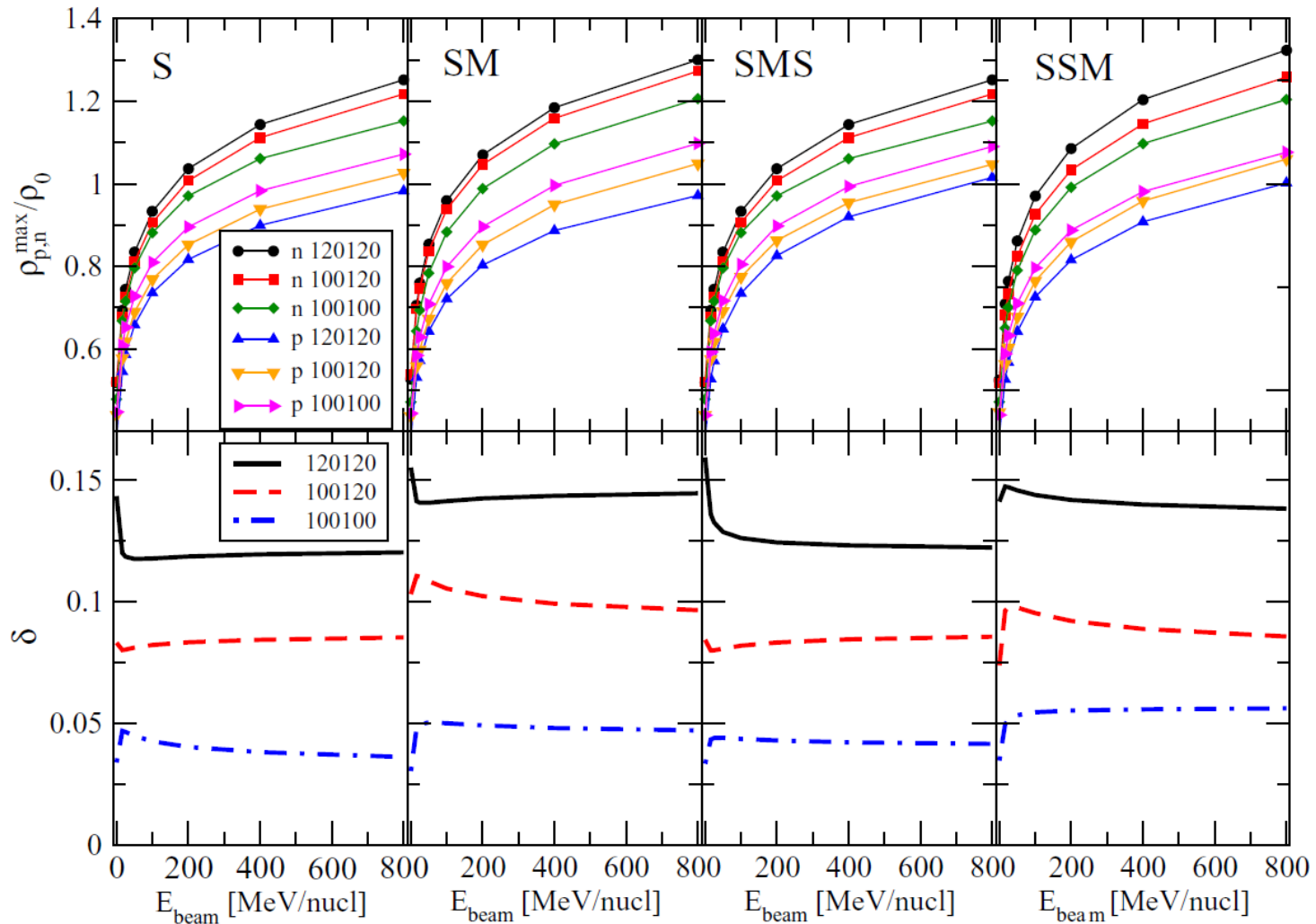


FIG. 6. The same as Fig. 4, but for Sn systems.

# Maximal density and corresponding $\delta$

**in comparison  
-medium energy-**

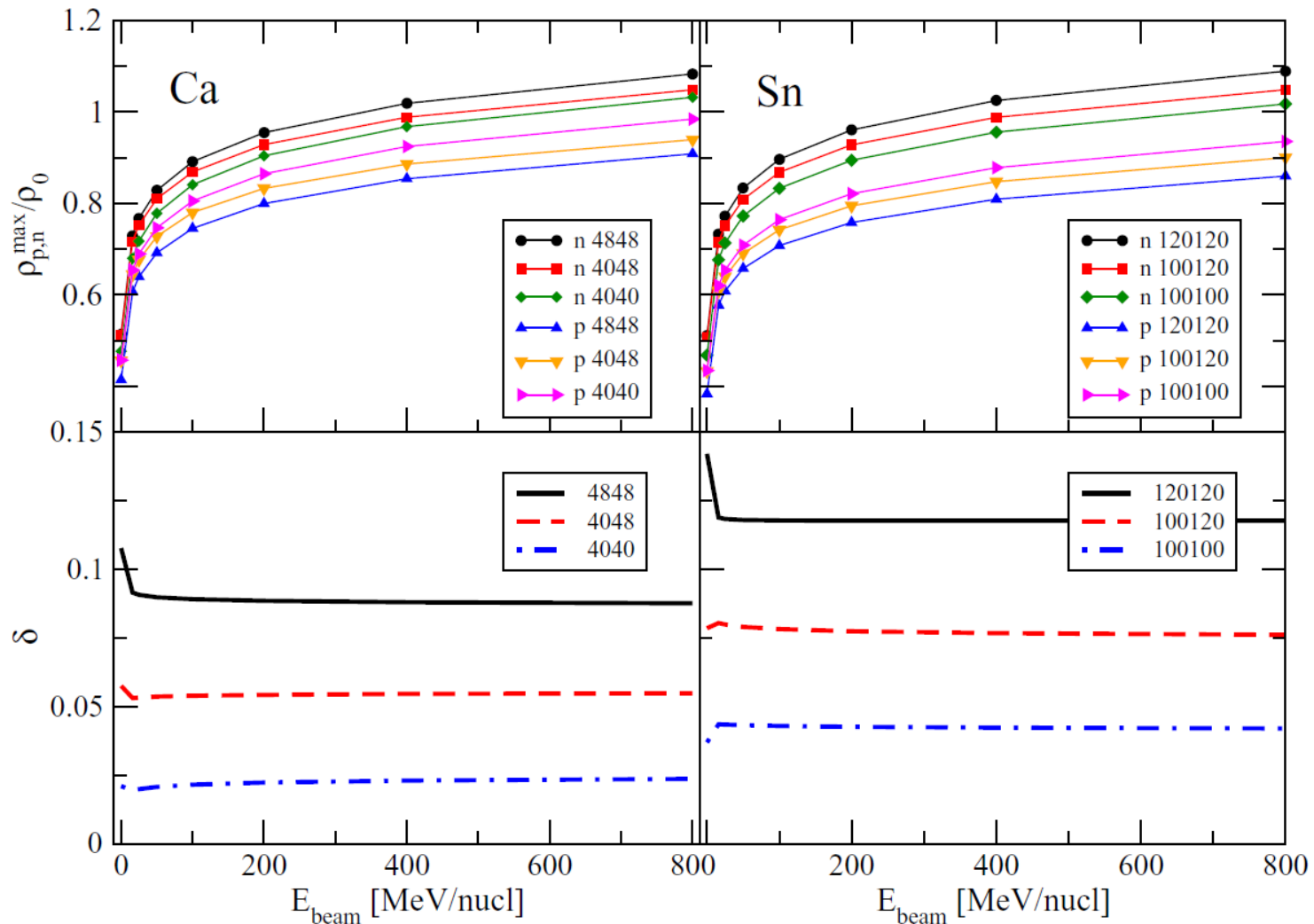


FIG. 7. Maximum neutron and proton densities in units of  $\rho_0$  (top panels) and corresponding values of asymmetry  $\delta$  (bottom panels), vs beam energy for Ca (left) and Sn (right) systems as calculated in Vlasov simulations with symmetry energy model S.

# Maximal density and corresponding $\delta$

**in comparison  
-low energy-**

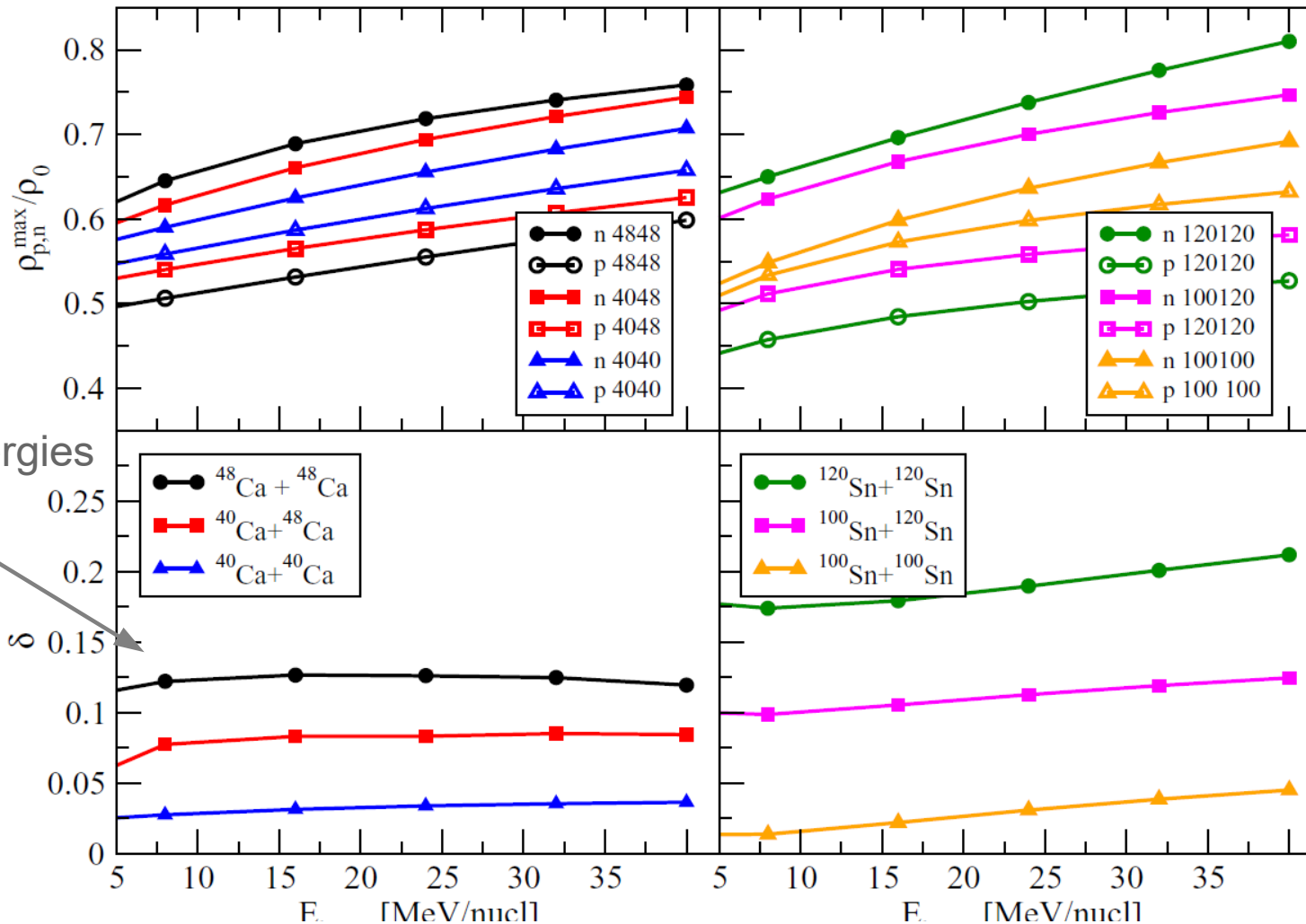


FIG. 8. Maximum neutron and proton densities in units of  $\rho_0$  (top panels) and the corresponding values of asymmetry  $\delta$  (bottom panels), vs beam energy for Ca (left) and Sn (right), from TDHF simulations.

# Ratio of maximal nucleon density -medium energy-

TABLE II. Ratio of maximal nucleon density reached at different beam energies  $E_{\text{beam}}$ , to maximal density in the initial state, for the Sn and Ca systems, as predicted in the pBUU, with the symmetry energy models S, SM, SMS, and SSM and in the Vlasov mode (V) with the symmetry energy model S. The columns are labeled with letters representing the version of the model, followed by mass numbers of the target and projectile combinations.

$E_{\text{beam}}$ MeV/nucl.	S			SM			SMS			SSM			V		
	120120	100120	100100	120120	100120	100100	120120	100120	100100	120120	100120	100100	120120	100120	100100
0	1.00	1.00	1.00	1.00	1.00	1.00	1.00	1.00	1.00	1.00	1.00	1.00	1.00	1.00	1.00
16	1.37	1.30	1.38	1.36	1.29	1.34	1.34	1.32	1.36	1.35	1.29	1.36	1.47	1.48	1.44
25	1.47	1.39	1.48	1.46	1.38	1.44	1.45	1.42	1.47	1.45	1.39	1.46	1.54	1.56	1.51
50	1.64	1.55	1.65	1.64	1.55	1.63	1.64	1.60	1.65	1.64	1.56	1.64	1.67	1.68	1.64
100	1.84	1.72	1.83	1.84	1.74	1.84	1.85	1.79	1.85	1.85	1.75	1.85	1.79	1.81	1.77
200	2.04	1.91	2.01	2.05	1.95	2.06	2.08	1.99	2.06	2.07	1.96	2.06	1.92	1.93	1.90
400	2.25	2.10	2.21	2.27	2.16	2.29	2.31	2.20	2.28	2.30	2.18	2.28	2.05	2.06	2.03
800	2.46	2.30	2.40	2.49	2.38	2.52	2.55	2.42	2.50	2.53	2.40	2.50	2.18	2.19	2.16
	4848	4048	4040	4848	4048	4040	4848	4048	4040	4848	4048	4040	4848	4048	4040
0	1.00	1.00	1.00	1.00	1.00	1.00	1.00	1.00	1.00	1.00	1.00	1.00	1.00	1.00	1.00
16	1.39	1.35	1.35	1.37	1.34	1.37	1.37	1.34	1.38	1.37	1.36	1.39	1.44	1.41	1.43
25	1.48	1.43	1.44	1.47	1.43	1.46	1.46	1.43	1.47	1.47	1.45	1.49	1.52	1.48	1.51
50	1.63	1.56	1.59	1.65	1.58	1.63	1.64	1.58	1.63	1.64	1.60	1.65	1.64	1.59	1.63
100	1.79	1.70	1.75	1.85	1.75	1.81	1.83	1.74	1.81	1.81	1.76	1.83	1.76	1.70	1.76
200	1.95	1.85	1.92	2.05	1.92	1.99	2.02	1.90	1.98	2.00	1.93	2.01	1.89	1.82	1.89
400	2.12	2.00	2.09	2.26	2.10	2.19	2.23	2.07	2.17	2.19	2.10	2.19	2.02	1.94	2.03
800	2.28	2.14	2.26	2.47	2.28	2.38	2.43	2.24	2.35	2.37	2.27	2.38	2.15	2.05	2.16



# Ratio of maximal nucleon density -low energy-

TABLE III. Ratio of maximal nucleon density reached at different beam energies  $E_{\text{beam}}$ , to maximal density in the initial state, for the Sn and Ca systems, as predicted by the TDHF model. The columns are labeled with mass numbers of the target and projectile combinations.

$E_{\text{beam}}$ MeV/nucl.	4848	4048	4040	120120	100120	100100
0	1.00	1.00	1.00	1.00	1.00	1.00
4	1.07	1.05	1.03	1.06	1.11	1.11
8	1.11	1.09	1.07	1.11	1.16	1.18
16	1.18	1.15	1.12	1.18	1.24	1.28
24	1.23	1.20	1.18	1.24	1.29	1.35
32	1.27	1.25	1.22	1.29	1.33	1.40
40	1.31	1.29	1.27	1.34	1.36	1.44

# Boundary of low- and medium energies

- isospin dynamics (chemical equilibration) defines its boundary  
... it is very fast compared to the other equilibration mechanisms

Charge equilibration upper-energy limit formula

$$\frac{E_{\text{CE,lab}}}{A} = \frac{\hbar^2(3\pi^2\rho_{\text{min}})^{2/3}}{2m} + \frac{e^2Z_1Z_2}{4\pi\epsilon_0r_0} \frac{A_1 + A_2}{A_1A_2(A_1^{1/3} + A_2^{1/3})}$$

$$\rho_{\text{min}} = \min_i \left( \frac{N_i \left(\frac{4\pi r_0}{3} A_i^{1/3}\right)^{-1}}{(1 - 3\bar{\epsilon})(1 + \bar{\delta})}, \frac{Z_i \left(\frac{4\pi r_0}{3} A_i^{1/3}\right)^{-1}}{(1 - 3\bar{\epsilon})(1 - \bar{\delta})} \right)$$

**Y. Iwata et al. PRL (2010)**

**This formula** says that

the bound energy is essentially determined by the **Fermi energy**,

and the additional kinematical effect (taken into account in the above) is not negligible

# Comparison to theory

TABLE I.  $E_{\text{CE,cm}}/A$  values [MeV] obtained by TDHF calculations compared to those obtained by transforming the results of Eq. (1) into the center-of-mass frame. For reference, the values obtained by the Fermi gas model with the standard parameter are also shown.

	Collision	TDHF (SLy4d)	TDHF (SkM*)	Equation (1)	Fermi gas
(i)	$^{208}\text{Pb} + ^{238}\text{U}$	$6.5 \pm 0.5$	$6.5 \pm 0.5$	6.91	9.46
(ii)	$^{208}\text{Pb} + ^{132}\text{Xe}$	$6.5 \pm 0.5$	$6.5 \pm 0.5$	6.50	9.03
(iii)	$^{208}\text{Pb} + ^{132}\text{Sn}$	$6.5 \pm 0.5$	$6.5 \pm 0.5$	6.36	9.03
(iv)	$^{208}\text{Pb} + ^{40}\text{Ca}$	$3.5 \pm 0.5$	$3.5 \pm 0.5$	3.66	5.14
(v)	$^{208}\text{Pb} + ^{24}\text{Mg}$	$2.5 \pm 0.5$	$2.5 \pm 0.5$	2.36	3.52
(vi)	$^{208}\text{Pb} + ^{24}\text{O}$	$2.5 \pm 0.5$	$2.5 \pm 0.5$	2.18	3.52
(vii)	$^{208}\text{Pb} + ^{16}\text{O}$	$1.5 \pm 0.5$	$1.5 \pm 0.5$	1.75	2.50
(viii)	$^{208}\text{Pb} + ^4\text{He}$	$<1.0$	$<1.0$	0.48	0.70
(ix)	$^{24}\text{Mg} + ^{24}\text{O}$	$5.5 \pm 1.0$	$5.5 \pm 1.0$	5.99	9.50

# Comparison to experiment

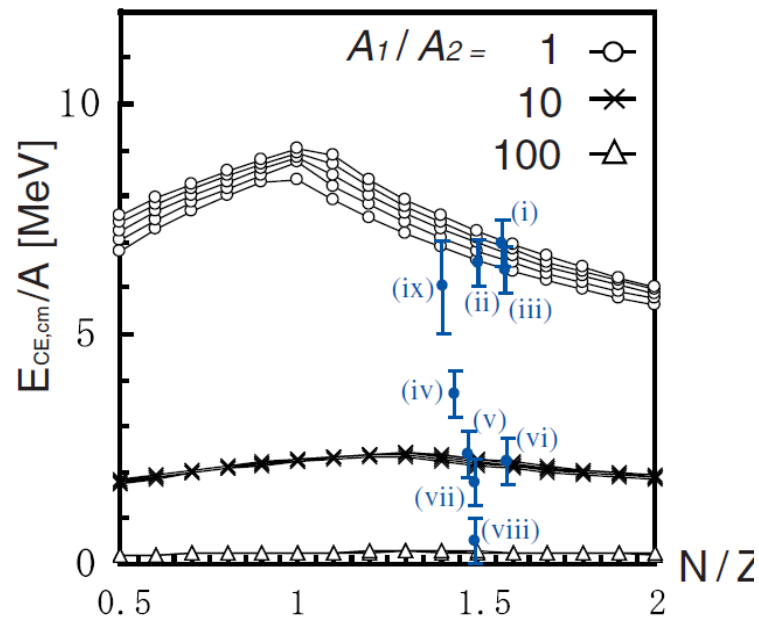


FIG. 2 (color online).  $N/Z$  dependence of  $E_{\text{CE,cm}}/A$  values [MeV] based on Eq. (1) in the center-of-mass frame, where  $A_1 > A_2$  is assumed without loss of generality. Values with different total masses  $A = 100, 200, 300, 400,$  and  $500$  are plotted for each  $A_1/A_2$ , which correspond to black lines from bottom to top in each group (the total mass difference is not noticed for the cases of  $A_1/A_2 = 10$  and  $100$ ), and the lines are drawn to guide eyes. Each TDHF calculation is shown as a blue bar, where the central points correspond to the value obtained by Eq. (1), and Roman numbers distinguish reactions shown in Table I.

Supportive results are recently reported in ...

Y. Zhang et al., Phys. Rev. C (R) (2017) **exp.**

L. Zhu et al., Phys. Lett. (2017) **exp.**

A. S. Umar Arxiv (2017) **thepr.**

# Boundary of low- and medium energies

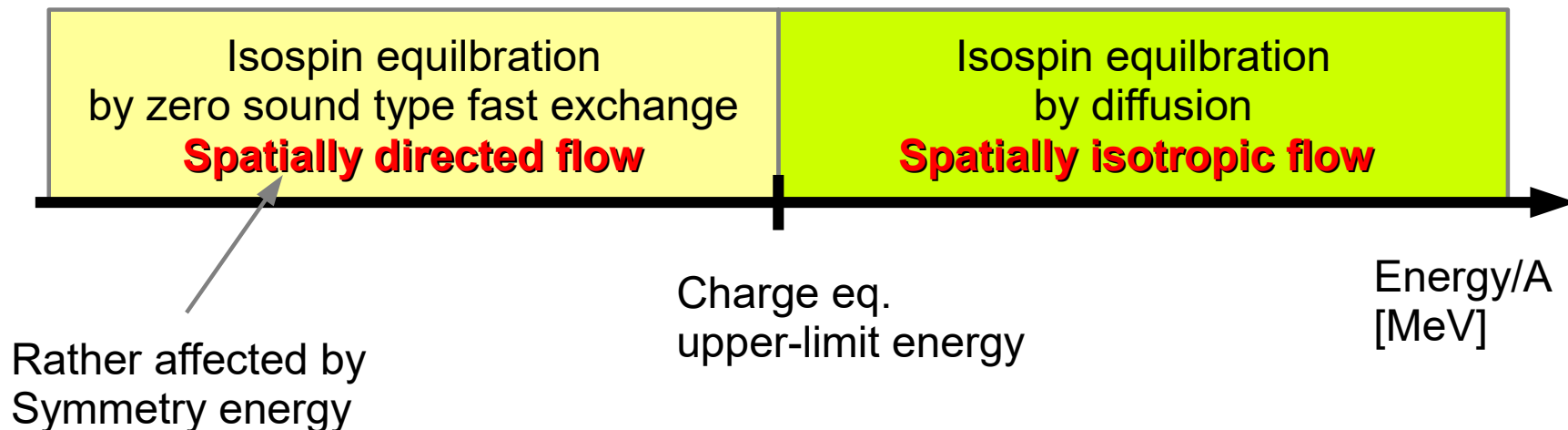
Charge equilibration upper-energy limit formula

$$\frac{E_{CE,lab}}{A} = \frac{\hbar^2(3\pi^2\rho_{min})^{2/3}}{2m} + \frac{e^2Z_1Z_2}{4\pi\epsilon_0r_0} \frac{A_1 + A_2}{A_1A_2(A_1^{1/3} + A_2^{1/3})}$$

$$\rho_{min} = \min_i \left( \frac{N_i \left(\frac{4\pi r_0}{3} A_i^{1/3}\right)^{-1}}{(1 - 3\bar{\epsilon})(1 + \bar{\delta})}, \frac{Z_i \left(\frac{4\pi r_0}{3} A_i^{1/3}\right)^{-1}}{(1 - 3\bar{\epsilon})(1 - \bar{\delta})} \right)$$

Y. Iwata et al. PRL (2010)

Roughly speaking



# Summary

- ◇ Maximal density achieved in low- and medium-energy HICs  
It is  $2.5 \cdot \rho_0$  in higher energies,  $1.4 \cdot \rho_0$  in low energies.
- ◇ Highest  $\delta$  is roughly equal to 0.17
- ◇ Maximal density is achieved in the first full-overlap.
- ◇ Maximal density **weakly** depends on ...  
Proton-neutron asymmetry **does depend** on ...  
initial cond, beam energy, system size, sym-energy models.

- ◇ The difference between two models are noticed:

– shell effect

...

